Remote and Ground Truth Spectral Measurement Comparisons of FORMOSAT III

Kira Jorgensen Abercromby
ESCG/Jacobs Sverdrup
2224 Bay Area Blvd, Houston, Texas, 77058
kira.abercromby-1@nasa.gov

Kris Hamada
Pacific Defense Solutions, LLC
590 Lipoa Pkwy, Kihei, HI 96753

Michael Guyote and Jennifer Okada
Boeing LTS, Inc.
1250 Academy Park Loop Suite 110, Colorado Springs, CO 80910

Edwin Barker
NASA Johnson Space Center
2101 NASA Parkway, Houston, TX 77058

ABSTRACT

FORMOSAT III are a set of six research satellites from Taiwan that were launched in April 2006. The satellites are in 800 km, 71 degree inclination orbits and separated by 24 degrees in ascending node. Laboratory spectral measurements were taken of outer surface materials on FORMOSAT III. From those measurements, a computer model was built to predict the spectral reflectance accounting for both solar phase angle and orientation of the spacecraft relative to the observer. However, materials exposed to the space environment have exhibited spectral changes including a darkening and a "reddening" of the spectra. This "reddening" is characterized by an increase in slope of the reflectance as the wavelength increases. Therefore, the model of pre-flight materials was augmented to include the presumed causative agent: space weathering effects.

Remote data were collected on two of the six FORMOSAT satellites using the 1.6 meter telescope at the AMOS (Air Force Maui Optical and Supercomputing) site with the Spica spectrometer. Due to the separation in ascending node, observations were acquired of whichever one of the six satellites was visible on that specific night. Three nights of data were collected using the red (6000 – 9500 angstroms) filter and five nights of data were collected using the blue (3200 -6600 angstroms) filter. A comparison of the data showed a good match to the pre-flight models for the blue filter region. The absorption feature near 5500 angstroms due to the copper colored Kapton multi-layer insulation (MLI) was very apparent in the remote samples and a good fit to the data was seen in all satellites observed. The features in the red filter regime agreed with the pre-flight model up through 7000 angstroms where the reddening begins and the slope of the remote sample increases. A comparison of the satellites showed similar features in the red and blue filter regions, i.e. the satellite surfaces were aging at the same rate.

A comparison of the pre-flight model to the first month of remote measurements showed the amount by which the satellite had reddened. The second month of data observed a satellite at a higher altitude and was therefore, not compared to the first month. A third month of data was collected but of satellites at the lower altitude regime and can only be compared to the first month. One cause of the reddening that was ruled out in early papers was a possible calibration issue.

1. INTRODUCTION

For many years spectroscopy has been used to determine the surface properties of remote targets. Recently, however, there has been a push to determine the materials on specific satellites, rocket bodies, and human-made debris. In this application, spectroscopy uses reflected light from a target illuminated by a continuum source (eg. the sun or a lamp) to produce a spectrum whose structure (absorption features and shape) can be indicative of a specific material composition. Since each material's spectrum is unique, material identification can be straightforward if its spectral features are well differentiated. Initially, studies showed that although a darkening of spacecraft materials was seen (and expected) over time, a change in the spectrum's slope beginning near 0.6 microns was also seen in almost all objects observed. One theory is that there is a contaminant on the material surfaces that changes the reflectance properties in the red region [1]. In order to study this theory, it was necessary to find satellites or rocket bodies that could be measured prior to launch so that the exact materials would be known. A set of satellites being launched by Taiwan were proposed and deemed to make an ideal case study. These spacecraft were chosen because the authors were able to take pre-flight measurements of the exact materials on the spacecraft so a more realistic comparison with the remote (telescope) data was possible. The details on both the laboratory and remote data collection are described later in sections 2 and 3.

The satellites observed in this study are a Taiwanese set of six satellites all called FORMOSAT III. FORMOSAT III are satellites based on the Orbital Sciences Corporation bus structure of a flat cylinder body with a nadir pointing boom and solar panels at the top of the spacecraft. Various views of the FORMOSAT satellite are shown in Fig. 1. Multi-layer insulation (MLI) covers the body of the spacecraft with a white nadir pointing boom. The solar panels are offset from the body at 59° degrees on one side, and 121° on the other in reference to the body. The solar panels do move around the y-axis (x-axis is down the body of the spacecraft) to track the sun, but keep the same angles to the body of the spacecraft. FORMOSAT III was launched April 15, 2006 into an orbit of 500 km circular altitude. The six identical satellites will take approximately 13 months to achieve a final circular orbit of ~ 800 km, 72° inclination, and separated by 24° in ascending node. The satellites are 1 m in diameter by 18 cm with a mass of 70 kg. The Space Surveillance Network numbers associated with FORMOSAT III are 29047, 29048, 29049, 29050, 29051, and 29052.

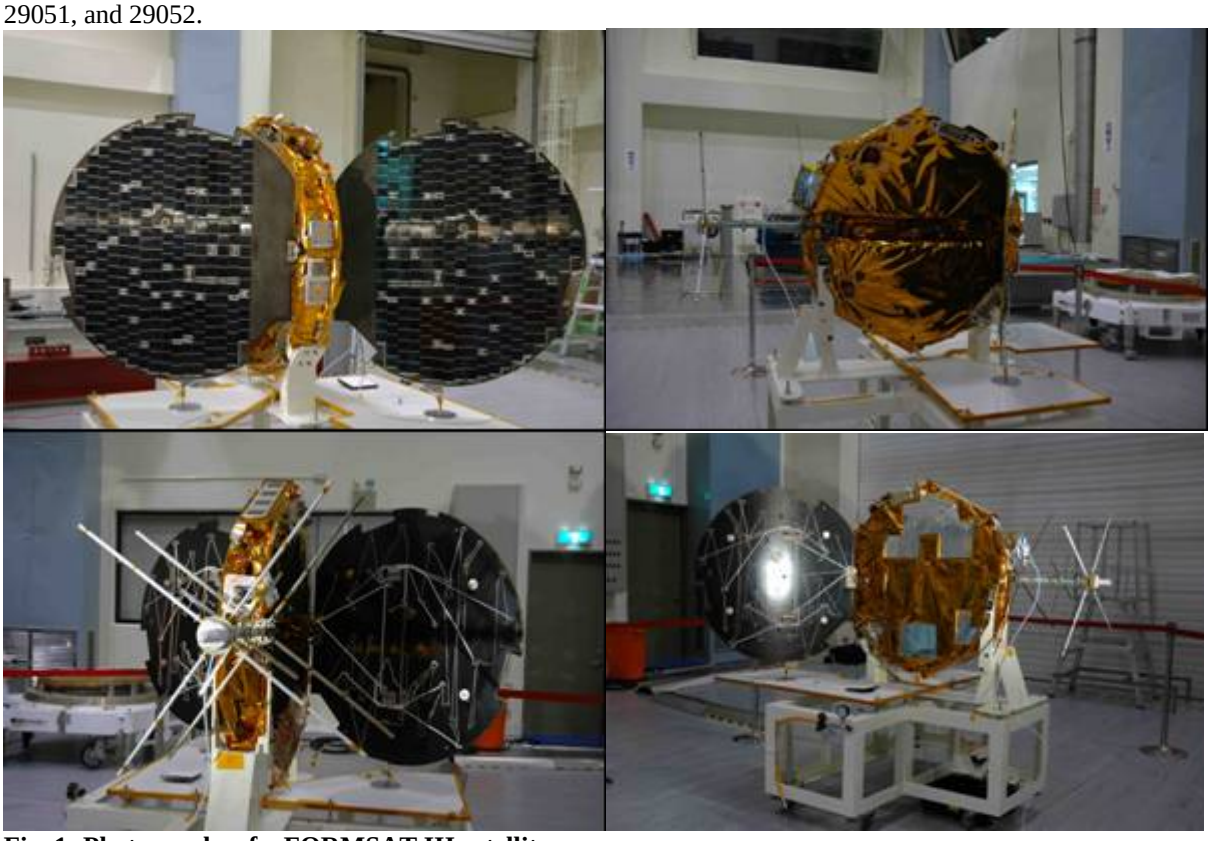

Fig. 1: Photographs of a FORMSAT III satellite

2. Laboratory Data

The team traveled to Taiwan to make pre-flight measurements prior to the satellites being sent to the United States for stacking and launching. All six satellites were launched at the same time. Spectral measurements were acquired with an Analytical Spectral Devices, Inc (ASD) field spectrometer that has a wavelength range from 0.3 to 2.5 microns (μm), a resolving power of 10 nanometers at 2 μm, and produces 717 total sample increments (simultaneous channels).

The satellite was enclosed in a clean room and, therefore, the scientists and the instrumentation followed the procedures laid out by the FORMOSAT team. All of the individual materials were tested, as well as broad views of the entire spacecraft, resulting in over 200 spectra. The satellite was oriented such that the normal nadir pointing of the satellite was toward a wall instead of the floor. This was advantageous for the data collectors because the solar panels were easier to measure in this configuration. All materials were considered flight ready, which means all the paints and coatings on the spacecraft were the same when we measured it as when the stack was launched.

The laboratory data was reduced using in-house data reduction processes [2], however, each material is expressed in absolute reflectance. All the material spectra can be combined linearly to make a model of the most probable distribution of surface materials and thereby predict the expected composite reflectance.

3. Remote Data Collection

All remote observations were taken using the 1.6 meter telescope and the spectrometer named Spica. Spica is an Acton SP-500i spectrometer with three angstrom resolution and three selectable gratings (although for this project the red and blue filters are used exclusively). The center wavelengths are 450 nm for blue grating and 750 nm for red grating. The band-passes are 320 – 660 nm and 600 – 900 nm for the blue and red gratings respectively. For calibration of the spectrometer, a mercury lamp is used for the blue wavelengths and a neon lamp is used for the red [3, 4]. The exposure time of each pass was varied to obtain the strongest signal to noise ratio possible. Some of the observations were exposed as short as 1 second while others were 10 seconds. Details of how the data were reduced have been well documented in previous papers [3, 4].

Table 1 shows what data was collected and when it was collected. The first set of observations was in late September 2006 where three satellites (29047, 29048, 29050) were observed using the blue filter. All three satellites where in the transition orbit near 500 km when the data was collected. Data collected in December 2006 spanned three nights - using the red filter on two of the nights and the blue filter one night. This data was all on one object (29049) that had made the transition to the final orbit at a semi-major axis of 793 km based on the two-line elements for those specific nights. The final observation set used for this paper was collected in early January 2007 on the same object in both the red and blue filter regimes. This object, 29051, was still in transition. To date, only one object, 29052, has not been observed with this system.

Table 1: Collection of data in terms of date, object, filter, and semi-major axis of object

Date	Object # (SSN)	Filter	Semi-major Axis (km)
09.30.2006	29047	blue	508
09.30.2006	29048	blue	513
09.30.2006	29050	blue	508
12.10.2006	29049	red	793
12.11.2006	29049	blue	793
12.12.2006	29049	red	793
01.13.2007	29051	red	512
01.14.2007	29051	blue	512

A unique aspect of these satellites from a research perspective is that they spent a variable but significant period of time at both 500 km and near 800 km semi-major axis (km). At 500 km, there is atomic oxygen in the environment,

whereas near 800 km the amount is negligible. This means there could be variations in the spectral response at various altitude regimes of these satellites based on the material interaction with the different environments.

4. COMPARISON OF DATA

4.1. Modeling the data

To combine spacecraft materials a linear mixing model can be used. The model is described by:

$$x = Sa + w,$$

where x is the observed spectrum, S is the set of component material spectra, a is the fractional abundances of each material, and w is the combination of observation noise and model uncertainty. In this case, S is known from the pre-flight measurements; however, determining the abundances of each material is an on-going issue.

Air Force models such as the Time-domain Analysis and Simulation for Advanced Tracking (TASAT) (developed by Air Force Research Laboratory (ARFL) and Northup Grumman) can be used to determine both the material type and abundance visible to the observer based upon ray-tracing and two-line element propagation. The major components on the FORMOSAT III were used to build a model in TASAT. An example of the TASAT model is shown in Fig. 2. This model is highly sensitive to lighting angles and material.

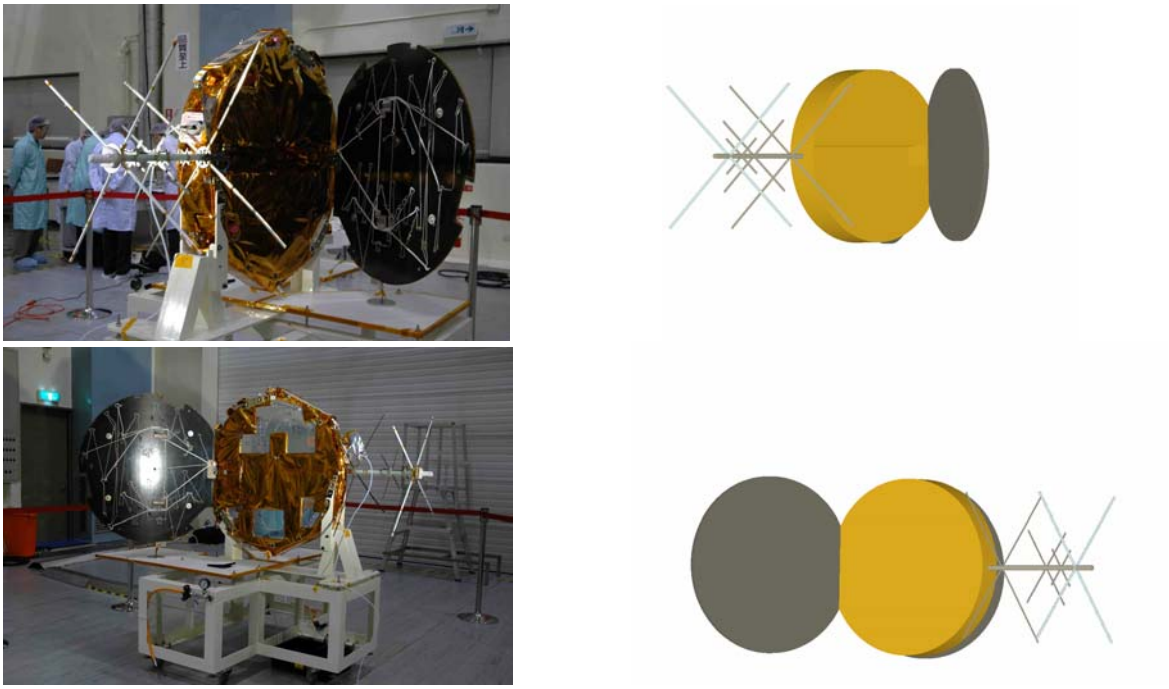

Fig. 2: Real Orientation compared with the TASAT modeling of FORMSOSAT III

An additional piece of information necessary to complete the model is how much light is being reflected from each component. Since this is not a standard output of TASAT, a model was built within MATLAB. This code determines where in the image the component lies, sums the intensity of the pixels from that component, and removes overlapping components from other materials.

The satellites have both an acute and obtuse angle between the satellite body and the solar panels. The acute angle is 59° while the obtuse angle is 121° with respect to the spacecraft body. It was determined using the two models that the orientation of FORMOSAT III satellites while over Maui was with the acute angle toward the sun. Four models will be used in the discussions that follow. All four models will use the breakdown of percentage of materials shown in Table 2.

Table 2: List of material abundances

Satellite Component	Abundance
Body	75%
Back of Solar panels	9%
Flat antenna crosses	9%
Cylindrical antenna cross	6%
Boom	1%

From previous investigations into the laboratory materials, it was shown that when the observer is viewing the acute angle of the spacecraft and the sun is directly to the right (simulating sunset), there is significant signal received from the MLI reflecting off the back of the solar panels [5]. A measurement of that reflection off the back of the solar panels was taken and is used Models 1 and 2 as the back of the solar panels component, while models 3 and 4 will use the back of the solar panel measurement without the MLI reflectance. Also, it has been shown that white paint tends to yellow in the presence of atomic oxygen [2]. These spacecraft were at 500 km for a few months, which is enough time to yellow the paint [2]. Models 1 and 2 will use white paint that has been weathered and appears more yellow than white for the cylindrical antenna cross and models 3 and 4 will use the original cylindrical antenna cross measurement.

The TASAT model uses Lambertian scattering for its Bi-directional Reflectance Distribution Function (BRDF), and this is not representative. By normalizing the materials to unity prior to the linear combination, the color effects on the brightness are absorbed into the abundances. Models 2 and 4 will normalize the materials to unity prior to the linear combination. Models 1 and 3 will combine the materials without normalization. Fig. 3 shows the four models used in this paper. The top figure shows models 1 and 3 since they are on similar scales, while the bottom figure shows models 2 and 4. The main difference in shape between the un-normalized and normalized models is the weakening of the white paint feature seen at 0.39 microns. Models 2 and 4 are very similar while model 1 appears more reflective than model 3 in the longer wavelengths.

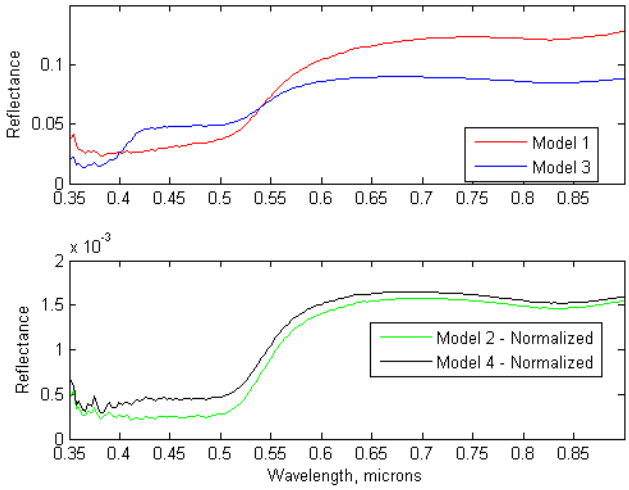

Fig. 3: Wavelength versus reflectance for the four models used in this paper

4.2. Blue filter data comparison

The blue filter is centered on 450 nm (0.45 microns (µm)) with a range of 320-660 nm (0.32-0.66 µm). The remote (telescope) data is very noisy and unreliable blueward of 0.35 µm. In order to plot the models and the remote data on the same chart, the data are ratioed to the reflectance value seen at 0.6 µm. Fig. 4 shows the comparison of the remote data from satellite 29050 with the models. The increase in reflectance beginning after 0.5 µm is due to the change in the MLI reflectance. The top graphs shows model 1 and 3 (the un-normalized models) and the bottom graph shows models 2 and 4 (the normalized models). Model 1 shows the best agreement with the remote data with only a slight disparity prior to 0.4 µm and after 0.6 µm. Model 3 shows a significant feature near 0.4 µm due to the

white color of the antenna crosses. However, as mentioned earlier, this feature is very weak in the normalized models. The disagreement after 0.6 µm will be discussed in the next section. All of the other blue data agree with the models within one sigma of error. This is a very positive result. Model 4 also agrees with the remote data quite well.

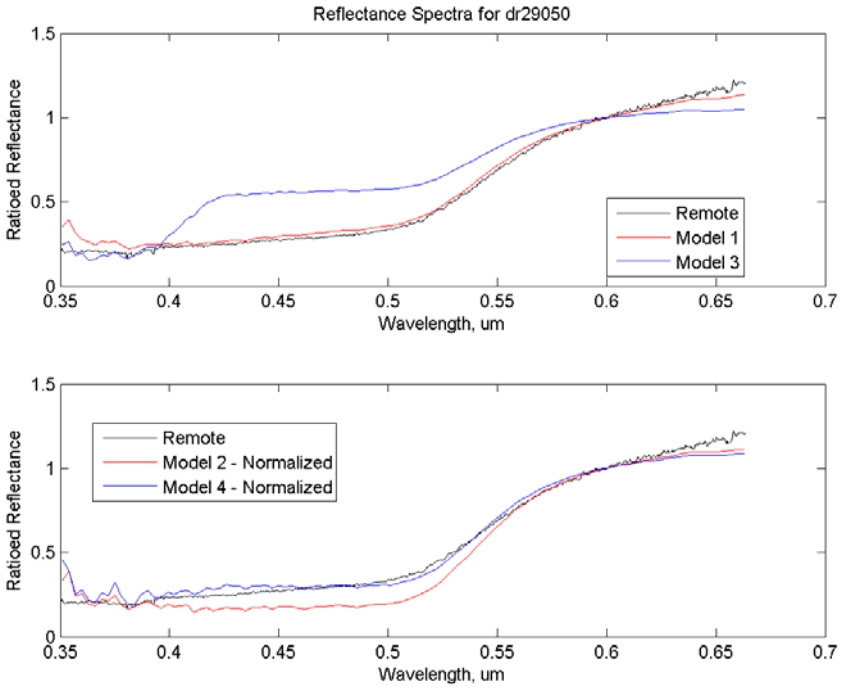

Fig. 4: Comparison of the blue filter data with the models

4.3. Red filter data comparison

Prior data collection has shown that as wavelength increases the slope of the remote data also increases [1, 4, 5]. Studies are under-way to determine the cause of the increase, or "reddening". However, this section will show an alternative method which allows the researchers to still obtain information from the reddened spectra.

Fig. 5 shows the data as collected. As with the blue data, the top figure shows the un-normalized models while the bottom plot shows the normalized models. As one can see, the models match the data well through 0.65 µm but then divert upwards in reflectance. This figure is just one example of this reddening. Astronomers studying asteroids and the lunar surface have seen this behavior as well [6]. In Clark and Roush [6], removing the continuum by division is found to be perfectly acceptable when examining specific absorption features. In Fig. 5, there is a broad feature centered near 0.85 µm that is difficult to see in the remote spectrum. However, if the continuum is divided out the feature is more apparent as seen in Fig. 6. The continuum end points for this plot are 0.65 to 0.9 microns. The feature that is being isolated may extend past 0.9 microns but since the data stops here, it is where the continuum must stop as well. In Fig. 6, models 1 and 3 are bracketing the remote data. In this case, the normalized models are a better match to the data - giving further justification for keeping both normalized and non-normalized models for the time being. The feature near 0.85 µm is due to aluminum in the materials and is seen in the models as well. Using the continuum confirms that the models are accurate for this satellite.

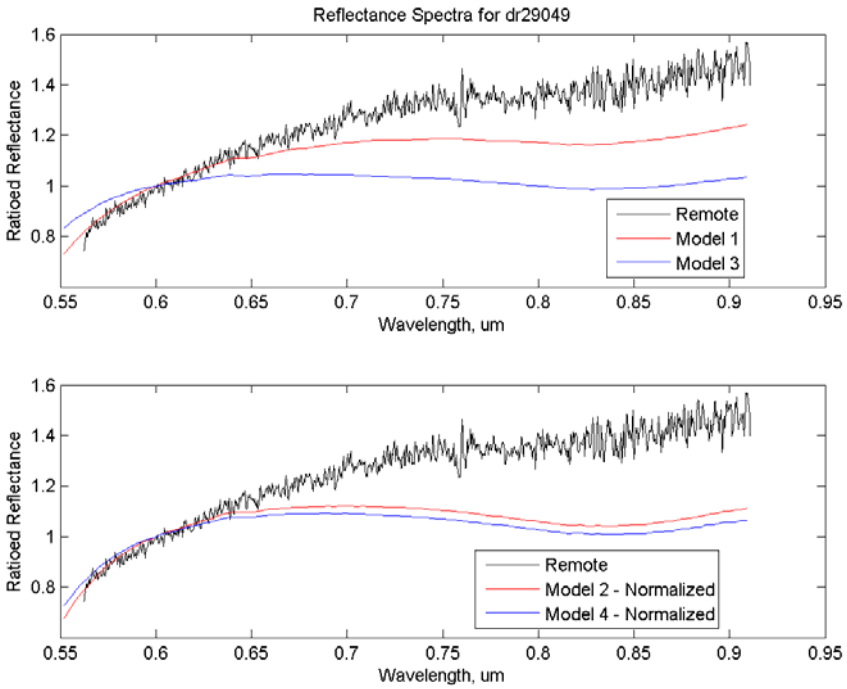

Fig. 5: Red filter data compared with the models

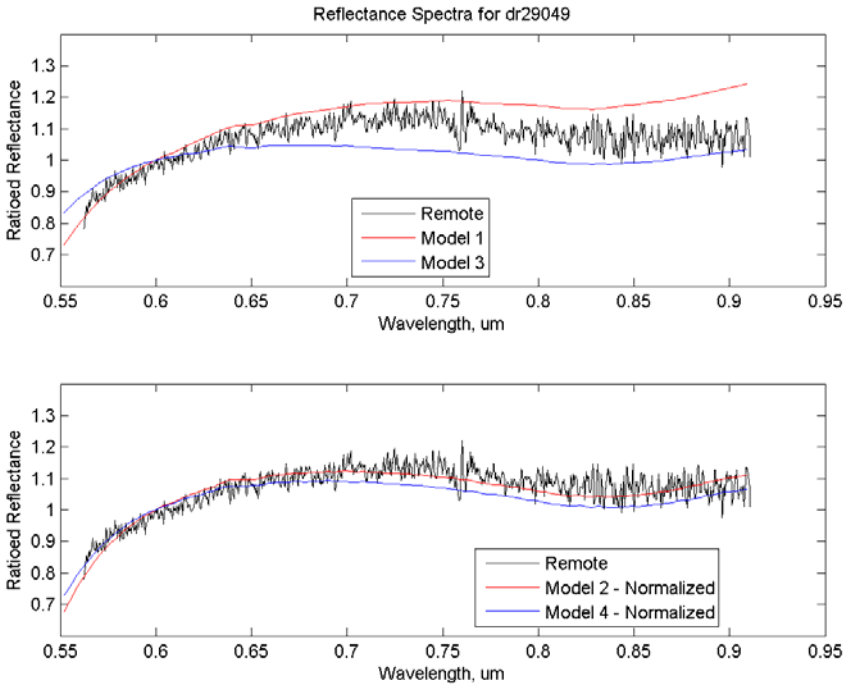

Fig. 6: Red filter data with continuum divided out as compared with the models

4.4. Reddening

4.4.1. Hapke Absorption Model

The reflective spectra of an object in space as described earlier has shown a tendency towards reddening (or increased relative reflectivity) at wavelengths greater than 0.65 microns. One theory, published by Hapke [7, 8], has shown that spacecraft materials can form a surface coating, which results in reddening due to the effects of electromagnetic diffusion and dispersion within this contaminant layer. Application of these processes to spacecraft materials is difficult due to the number of unknown variables and the uncertainty in determining how the particles attach to the surface. One theory is that once the object is in space, oxygen vacating the surface material leaves places where the contaminant can attach to the surface. Re-introduction of the material to an oxygen rich environment breaks the bond with the contaminant and restores the original oxygen. For this theory to be proven, the next step is to apply the Hapke model.

4.4.2. Analysis Approach

As discussed in a previous paper [8], it was conjectured that information on surface contamination could be gained from utilizing the Hapke diffusion relationships to analyze the observed spectral reddening. The task is difficult, given that there are many variables associated with the reddening equation. Also, when analyzing the particle distribution contribution (θ), the complimentary relationship of variables introduces another problem because the same spectral result can be obtained by increasing one variable whilst decreasing another in a like proportion.

The analysis technique involves the following steps: 1) calculating a difference (or reddened spectrum) between laboratory and space observations, 2) altering a "flat" spectrum (utilizing the Hapke relationships) such that it matches the reddened spectra, and 3) selecting an appropriate set of variables which produce the reddened spectra. A typical target spectral curve is chosen from among spectra that have been analyzed and a selected searching technique is applied. It is designed to “tune” the Hapke equations such that the resulting output spectral curve matches the target spectral curve.

The spectral match is performed by Particle Swarm Optimization (PSO), a stochastic technique which operates by initializing a solution space with a number of random solutions, computing the error for each solution, and updating each solution. The updating process involves keeping track of each particle state and noting the particle with the best fit to the target spectrum. The actions of all of the other particles are then altered so as to cause them to move towards the solution space obtained by the best fit particle. The process is judged complete when the error is brought below a selected minimum bound, which is user defined. For step 1, it was found that the difference between the two spectra produced a very noisy solution for which the particle swarm had difficulty processing. For this section only, a polynomial best-fit smoothed spectrum was computed from the differenced spectrum. The swarm search technique utilizes the smoothed difference spectra as its target. Examples of the smoothed data for each of the models are shown in Fig. 7. The left image shows data of a satellite at 800 km taken in December 2006 while the right image shows an object still at 500 km and taken in January. Note that the wavelength scales are slightly different in length such that the right plot is longer than the left. Even though the measurements are taken with the same instrument, some evenings have nosier data near the end of filter regime and are thus, cut off earlier. However, three of the models show similar shapes and strengths of reddening (model 2, 3, and 4) while model 1 shows a better agreement with the reddened remotely acquired spectrum. Even though model 1 has a lower level of reddening it still is reddened. It appears as if the reddening is tailing off from the models, however, this may be due to the absorption feature seen previously at 0.85 μm. The models also show good agreement in shape between the December and January data; however, the strength of the curves are greater in the January data. This could mean the reddening is increasing with age, or that there is more reddening shown at 500 km as compared to 800 km altitude regimes. This will be studied in future work.

The second step involves altering the Hapke equation variables such that the initial spectrum (which starts out as a flat line with optional absorption characteristics programmed in) matches the smoothed difference spectrum. The spectral match is again performed by PSO.

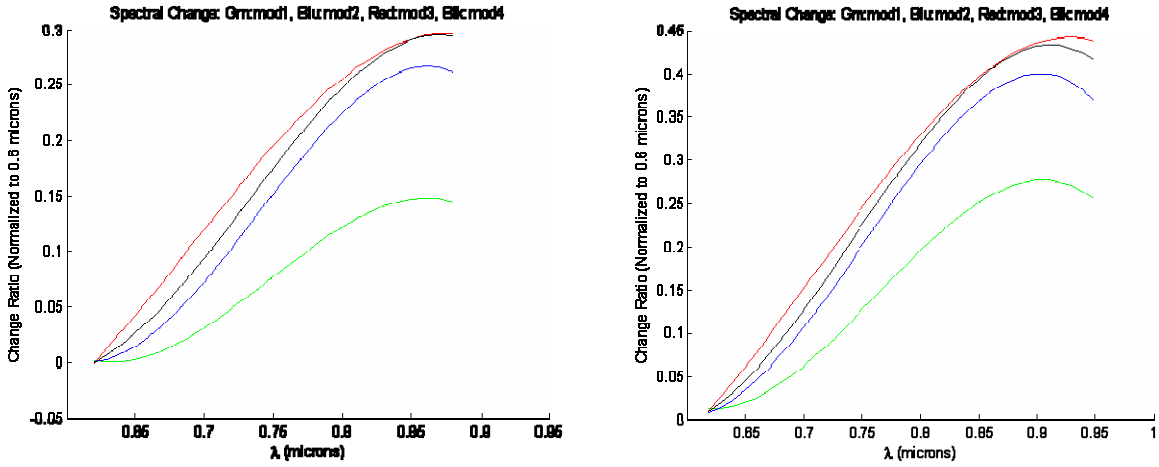

Fig. 7: Smoothed difference spectra for each model as compared to two days of data. The left image shows data of a FORMOSAT III satellite 29049 at 800 km taken in December 2006, and the image on the right shows FORMOSAT III satellite 29051 taken in January 2007 but the objects altitude was still 500 km.

Our preliminary data runs have not produced acceptable results, due to the fact that the search variable space was deemed to be too large. Multiple runs do not appear to produce converging results. However, the authors are researching existing variable space data to determine whether or not we can limit the bounds of some of the parameters (particle densities, coating depths) - which influence the overall reddening slope, along with acquiring more accurate data on the refractive indices of the coating particles - which influence the change in absorption features.

5. CONCLUSIONS

Although the cause of spacecraft reddening remains unresolved, great progress has been made. Measurements of a set of satellites were made pre-flight so that material composition was known definitively. However, it was shown that some materials change in reflectance over time and one or two of the materials needed to be augmented. To test the variation in materials, two models were made that varied in materials based on both pre-flight and space weathered samples. Additionally, to remove biases in the derivation of percentage of materials at each orientation, one model normalized the materials prior to linear combination and a second model did not normalize prior to linear combination. In the end, four models were created to compare to the remotely acquired spectra.

Using the blue filter, model 1 (non-normalized and space weathered materials) was the best fit to the data. However, model 4 (normalized and pristine materials) showed good agreement as well. Overall, the data from the blue filter agreed quite well.

The red filter data proved to be more problematic. As expected, a reddening had occurred of the surfaces making it difficult to determine location and strength of specific absorption features. Dividing out by a continuum, the absorption feature was matched with the aluminum in the ground sample data. Although unsuccessful, an attempt was made to determine the nature of materials which may be adhering to spacecraft surfaces and causing spectral reddening. Future work will further evaluate the different variables necessary for the Hapke model.

6. ACKNOWLEDGEMENTS

The authors would like to thank Dennis Liang for his persistence in trying to get the remote data. Also, we would like to thank all those as NSPO, especially Toni Tsai, for access to the FORMOSAT III spacecraft. Part of the funding for this project comes from the Air Force Office of Scientific Research (AFOSR) and we thank Kent Miller for his continued support as well as being the connection and contact for the FORMOSAT III observations.

7. REFERENCES

1. Guyote, M., Abercromby, K.J., and Okada, J., *Using Space Weathering Models to Match Observed Spectra to Predicted Spectra*, 2006 AMOS Technical Conference, Wailea, Maui, Hawaii, September 2006.

2. Jorgensen, K., Using Reflectance Spectroscopy to Determine Material Type of Orbital Debris, Ph.D. Thesis, University of Colorado, Boulder, May 2000.

3. Nishimoto, D.L. Kervin, P., Sydney, P., Hamada, K., and Africano, J., Spectroscopic Observations of Space Objects and Phenomena using Spica and Kala at AMOS, *Proceedings of SPIE*, **Vol. 4490B**, San Diego, California, 29 July - 3 August 2001.

4. Jorgensen, K., Okada, J., Guyote, M., Africano, J., Hall, D., Hamada, K., Barker, E., Stansbery, G., and Kervin, P., Reflectance Spectra of Human-made Objects, *2004 AMOS Technical Conference*, Wailea, Maui, Hawaii, 8 – 12 September 2004.

5. Abercromby, K.J., Okada J., Guyote, M., Hamada, K., and Barker, E., Comparisons of Ground Truth and Remote spectral Measurements of FORMOSAT and ANDE Spacecraft, *2007 AMOS Technical Conference*, Wailea, Maui, Hawaii, September 2006.

6. Clark, R.N. and T.L. Roush, Reflectance Spectroscopy: Quantitative Analysis Techniques for Remote Sensing Applications, *J. Geophys. Res.*, **89,** 6329-6340, 1984.

7. Hapke, B, Space Weathering from Mercury to the asteroid belt, *Journal of Geophysical Research*, **Vol. 106**, No E5, Pages 10,039-10,073, May 25, 2001.

8. Abercromby, K.J., Guyote, M., Okada, J. , and Barker, E., Applying Space Weathering Models to Common Spacecraft Materials to Predict Spectral Signatures, *2005 AMOS Technical Conference*, Wailea, Maui, Hawaii, September 2005.